New Interpretation of Resonant Photoemission Spectra of Solid Actinide Systems

S. L. Molodtsov,[1,*] S. V. Halilov,[2,3] Manuel Richter,[4] A. Zangwill,[3] and C. Laubschat[1]
[1] *Institut für Oberflächenphysik und Mikrostrukturphysik, TU Dresden, D-01062 Dresden*
[2] *NIST, Gaithersburg MD 20899-8412, USA*
[3] *School of Physics, Georgia Institute of Technology, Atlanta GA 30332, USA*
[4] *Dept. of Theoretical Solid State Physics, IFW Dresden, P.O. Box 270016, D-01171 Dresden, Germany*

It is shown that angle-resolved valence-band photoemission (PE) spectra of epitaxial close-packed films of U metal may correctly be described within a one-step model of PE based on a band description of the U $5f$ states. It is found that a cross-section minimum at $h\nu = 90$ - 94 eV, which previously was assigned to a Fano antiresonance at the $5d \rightarrow 5f$ excitation threshold, is mainly caused by a Cooper-minimum behavior. Analogous cross-section variations in the region of the $5d \rightarrow 5f$ resonances were obtained for a series of other solid actinide systems. The reported results have severe consequences for the general interpretation of resonant PE data.

79.60.-i; 79.60.Bm; 71.20.-b

Cross-section variations as a function of photon energy are frequently used to discriminate between contributions of different electronic states to photoelectron spectra of solids. A rather dramatic effect is exploited in resonant photoemission (PE): Here, the excitation into the PE continuum is coupled to a transition into a discrete intermediate state followed by autoionization leading to a Fano resonance in the photoionization cross section [1–3]. On resonance, the emission intensity is strongly enhanced by a constructive interference of the channels, while, off-resonance, it is decreased by a destructive interference. Since the channel mixing entails an Auger matrix element the resonance depends strongly on the spatial localization of the states involved [4]. Particularly large effects have, therefore, been reported for the $4f$ and $5f$ states of rare-earth's (RE's) and actinides, respectively [5–9].

Due to their rather localized character, the f states are mainly responsible for the magnetic properties of these materials. On the other hand, interactions of f electrons with valence-band states lead to fascinating many-body phenomena like Kondo effect, mixed-valence or heavy-fermion behavior [10]. Resonant PE offers a promising tool to study such phenomena. Interpretation of resonance PE data may lead, however, to misleading conclusions, if not all arising effects are taken into consideration. It was found, for example, that PE signals related to nonequivalent atomiclike $4f$ electronic configurations in RE's reveal different enhancements across the $4d \rightarrow 4f$ excitation threshold [11]. Resonant PE response from the $5f$ states, which exhibit bandlike properties in some actinides and their compounds [9,12,13] may be more affected by solid-state phenomena like, e.g., the real band structure of the initial state including hybridization with valence states of other angular-momentum characters or crystal symmetry selection rules for the dipole transitions between initial and both final PE state and intermediate state of the autoionization channel. A simple physical interpretation of the resonant phenomena for single atoms has been given earlier within a time-dependent density-functional technique [2]. Based on the same approach, the effect of solid-state hybridization on the resonant photoemission process in solid uranium has been modelled by consideration of a single uranium atom embedded in a spherical drop of jellium [3]. The resonant photoemission is imposed by transitions between the ground-state configuration of U ($5d^{10}5f^3$) and the multiplets of the core-excited $5d^9 5f^4$ configuration. In particular, the absorption of a single U atom is totally dominated by three transitions, located at 96, 102 and 106 eV.

Present consideration is focused on the varation of the off-resonance photoemission cross-section in the broad range of photon energies, shown to have a very strong dependence from the spatial distribution of the $5f$ states, which essentially interferes with the resonance processes as well. In atomic physics, it has been shown [14] that the strong variation of the cross section can be caused by a node in the radial part of the initial-state wave function, which may lead to the cancelation of the dipole matrix elements for electron transitions into oscillating free-electron-like final states (Cooper minimum, CM). Energy positions of the CM were calculated for a large variety of elements from the periodic table including actinides [15]. Thereby not more than one CM was obtained for each atomic shell considered and the CM for the $5f$ shells were found to be well separated in energy from the $5d \rightarrow 5f$ resonances. In contrast to the atomic case a series of CM was recently found for $4d$, $5d$, and $5f$ upper shells in a number of elemental metals [16]. In solid actinide systems, in particular, the CM may overlap the energy region of the $5d \rightarrow 5f$ resonant excitation.

In this contribution we discuss an application of resonant PE to U metal, where the $5f$ states reveal dispersion in the binding energy (BE) range between 0.5 eV and 2 eV and their itinerant description is appropriate [13]. We performed density-functional calculations of photoelectron energy distribution curves (EDC's) based on an one-step model of PE for close-packed (*fcc* or *hcp*) phases of U metal. Good correspondence between theory and ex-

periment over a wide range of photon energies is obtained for thin films of *hcp* U metal. The calculated EDC's are in agreement with the experimental spectra also in the energy region of the $5d \rightarrow 5f$ resonance (up to $h\nu \approx 103\,eV$), although mixing of the single-partical direct PE channel and the many-body autoionization channel has not been taken into account in our model. We show that an intensity drop of the Fermi-level (E_F) peak at 90 - 94 eV and its enhancement at 98 eV photon energy, that previously had solely been assigned to the Fano resonance [7–9,17–20], are mainly caused by the solid-state CM, while resonance effects are only a minor contribution here. Similar results obtained for the polycrystalline U metal and the intermetallic compound UPd_3 suggest that crystal symmetry and change of lattice parameters have a rather small effect on the PE intensity variations in the photon energy range considered. As in the case of the U systems, our cross-section calculations for *fcc* Pu metal disclose the solid-state CM, which is located close to the $5d \rightarrow 5f$ excitation.

Ordered close-packed films of U metal were prepared by *in-situ* deposition of U onto a liquid nitrogen cooled W(110) substrate followed by annealing of the "as deposited" system (for details see Ref. [13]). PE experiments were performed at the Berliner Elektronenspeicherring für Synchrotronstrahlung (BESSY) using radiation from the plane-grating monochromator beamline SX700/II. Photon energies were varied within the range from 60 eV to 145 eV. The incidence angle of photons was chosen to be 35° relative to the sample surface. A rotatable hemispherical electron-energy analyzer was employed to take PE spectra with an overall-system energy resolution of about 100 meV (FWHM) and an angular resolution of 1°. The base pressure in the experimental set-up was in the range of 1×10^{-8} Pa.

A series of normal-emission valence-band PE spectra taken from an ordered U film at different photon energies is shown in Fig. 1. The spectra are normalized to the photon flux. All spectra except those taken just below the $5d \rightarrow 5f$ excitation threshold at $h\nu = 90\,eV$ and 94 eV reveal similar triangle-like shapes characterized by a sharp peak at E_F and a series of less intense features within the first 2 eV below E_F. While the former reveals no clear dispersion, the higher-BE features change their positions with photon energies. At $h\nu = 90\,eV$ and 94 eV, the Fermi-level peak becomes suppressed, whereas the features at higher BE's are much less affected. The experimental data were compared to normal-emission EDC's for (0001) and (111) surfaces of *hcp* and *fcc* U metal, respectively, calculated for various in-plane nearest-neighbor distances a in the range of values $a = (3.2 \pm 0.2)$ Å estimated from the LEED experiment. In all cases better agreement between experimental and theoretical results was obtained for the *hcp* arrangement. The applied relativistic layer KKR method (see, e.g., Ref. [21] and references therein) has the advantage to account for surface contributions to the PE signal. In the calculations, use was made of the local density approximation (LDA) and the surface was described by a simple truncation of the bulk. The final states were described by time-reversed LEED states. In order to account for the finite experiment angular resolution the calculated PE signals were integrated within a cone of 2°.

The calculated EDC's for an ideal *hcp* structure and $a = 3.0$ Å are presented in Fig. 1. "As calculated" EDC's were broadened by a Gaussian to account for a finite experimental resolution. Linear dependence of lifetime broadening from binding energy in a form 0.05 (BE - E_F) was assumed. All theoretical EDC's were consistently normalized to equal intensities of the simulated and the experimentally observed Fermi-level peaks at $h\nu = 65\,eV$. Note, that in contrast to the experimental spectra the theoretical EDC's contain no background of inelastically scattered electrons. For all PE spectra shown in Fig. 1, good agreement between experimental and calculated dispersions and intensities is obtained.

Dispersions along the Γ-A direction in the Brillouin zone of the *hcp* U are shown in the inset in Fig. 1. There are five experimental occupied bands in the region between E_F and 2 eV BE, which are correctly reproduced by the calculations. According to our eigenvector analysis all electronic states shown in the inset reveal predominantly f character, although its amount decreases from 90% for the flat bands calculated within the first 0.5 eV below E_F to about 50% for the lower laying bands with more pronounced dispersion. Except the photon-energy range approximately from 90 to 94 eV our calculations predict larger transition probabilities from the more localized Fermi-energy $5f$ states than from the $5f$ bands at higher BE's, that is in agreement with the experimental observations. At 90 eV and 94 eV photon energy, the intensity of the Fermi-level peak becomes suppressed, an effect that previously had been attributed to a destructive Fano interference of direct PE with a $5d \rightarrow 5f$ autoionization channel [7–9,17–20]. Surprisingly, our theoretical EDC's reproduce this intensity variations, although channel mixing was not taken into consideration in the calculations. Obviously, the usual interpretation of this phenomenon in terms of only Fano antiresonance is not complete. This conclusion is of high importance for the interpretation of resonant PE studies of U systems, in particular, if the degree of localization of the $5f$ states is determined from the Fano-profile assymetry parameter, which value strongly depends on the depth and energy position of the intensity drop in the preresonance region.

To understand the drop in PE intensity at E_F we analyzed, first, the angle dependent part of the dipole matrix element and found that from their symmetry properties all five valence bands (see inset in Fig. 1) are expected to contribute to PE spectra. According to dipole angular-momentum character selection rules, for f states only

transitions into d or g final states are allowed. Our calculations for the *hcp* U reveal a certain depletion of those upper d- and g-partial electronic densities of states, that are allowed by crystal symmetry for the transitions from the $5f$ occupied bands, in the energy range from 90 to 94 eV above E_F. However, similar experimental intensity variations of the Fermi-energy feature were observed for polycrystalline samples of U metal [7,18] and for a large variety of U compounds [7–9,17,19,20]. It is very unprobable that all studied U systems, independent of their composition and crystal symmetry, reveal similar depletions in the electronic structure of the empty states at such high energies.

Thus, the energy dependence of radial dipole coupling between valence $5f$ states and continuum εd and εg states is suspected to cause the system-independent intensity variations. The radial wave functions entering the related matrix element $M^r_{5f\to\varepsilon g,\varepsilon d}$ are obtained by outward integration of the one-electron Dirac equation at fixed energies $\varepsilon_{5f} = E_F$ (initial state) and ε (final state), respectively, and by matching to spherical functions at the Wigner Seitz (WS) cell radius, $r = r_{ws}$. The potential used in the Dirac operator is obtained from a self-consistent relativistic linearized muffin-tin orbital LDA calculation. The values obtained for transitions from the $5f$ initial states into εd final states are more than one order of magnitude smaller than those for the transitions into the εg states and, therefore, are not accounted for in the further consideration.

For free atom bound states, the amplitudes of the electron wave functions decay exponentially at large distance to the nucleus, and the transition matrix elements are calculated by integration over the whole space. In a solid, periodic Bloch states are formed and for direct transitions all translationally equivalent WS cells give the same contributions to the integral. Therefore, the upper limit of integration of renormalized wave functions is changed now to the r_{ws} value [16]. As a result, in contrast to the free atom case, our calculations reveal several minima of $|M^r|^2$ for U metal (two in the region 60 eV $\leq$ hν $\leq$ 350 eV, see Fig. 2). Note that the results presented in Fig. 2 have only a qualitative meaning: They do not include the joint density of states as well as surface effects or crystal symmetry selection rules, which are accounted for in the complete calculations, Fig. 1. For r_{ws} = 1.7 Å (corresponding to *hcp* U with a = 3.0 Å) a low laying minimum is found in the region of the Fano antiresonance, whereas a high laying minimum is observed at a photon energy of 265 eV that is approximately 50 eV above the convential CM calculated for U *atoms* [15]. If the excitation energy is close to the energy region of the CM in U metal a node of the radial wave function of the continuum PE final state shifts with increasing energy toward the outer extremum of the $5f$ wave function (inset in Fig. 2) causing alternating in sign (marked in the inset) contributions to the radial matrix element. Under certain conditions (compare final states reached with 55-eV and 94-eV photons) this may lead to a cancelation of the M^r. In contrast to narrow $5f$ bands at E_F, broad $5f$ hybrid bands at higher BE's do not reveal pronounced CM intensity variations. Smearing of the solid-state CM's for bandlike hybridized electronic states is a well-known phenomenon [22], that can be explained by contributions into PE intensity of valence electrons with different angular momentum character.

Within our theoretical approach we simulated experimental results for polycrystalline U metal [7] by integrating the calculated PE intensities within a rather large escape cone of 25° (not shown). We performed also calculations of matrix elements (Fig. 2) and PE intensities (Fig. 3) for intermetallic compound UPd_3 [17]. Like in the experiments [7,17] in all cases, drops of the $5f$-derived PE at E_F were obtained in the region of h$\nu \approx$ 90 - 94 eV. Our calculations reveal the common behavior of cross-section variations for various U systems, that are characterized by different crystal symmetries, specific band structures or crystal-symmetry selection rules related to properties of the angular part of the wave functions. This result can be understood by the fact that the CM behavior is mainly determined by the initial radial wave function that is of course very much similar in all solids considered. It explains also similar intensity variations with minima of the $5f$ signal at about 92 eV photon energy followed by an increase of the $5f$ PE cross section at h$\nu \simeq$ 98 eV observed for a series of other U systems [7–9,17–20].

Should the Cooper mechanism be regarded as the only reason for the observed intensity variations in the considered region of photon energies? The contribution of the Fano resonance to the cross section can be estimated from a direct comparison of the calculated and experimentally observed Fermi-level peak intensities as a function of photon energy. The experimental (open circles) and the theoretical (solid circles) constant initial states (CIS) profiles for *hcp* U and UPd_3 are shown in Fig. 3. As evident from the figure, the observed intensity variation in the energy range from about 60 eV to 103 eV can be predominantly explained by direct PE. An additional enhancement of the signal at hν = 98 eV, which may be assigned to resonant excitations, does not exceed 20 % of the total intensity. In all studied U systems the situation is reversed for the photon-energy range from 105 eV up to about 120 eV. Here, the calculated direct PE response is only a minor contribution to the measured intensity that indicates in fact the Fano-resonance behavior. The CIS profiles depicted in Fig. 3 can be compared to a x-ray absorption spectrum (XAS) taken for *hcp* U in a partial electron yield mode with 1-eV kinetic energy electrons. Note, that details of the lineshape of the XAS spectrum reflects a rather complicated broad multiplet structure of the $5d^9 5f^{x+1}$ intermediate state that do not directly relate to the $5d$ spin-orbit splitting [19]. In difference to

the CIS experiment, not only direct $5f \rightarrow \varepsilon g$ and resonant excitations but also PE from the rest of the valence band, $6p$, $6s$, and $5d$ core levels as well as Auger electron channels contribute to the XAS spectrum. Since the latter contributions are not influenced by the Cooper mechanism, the relative intensity in the energy region 90 - 103 eV as compared to the signal in the region 105 - 120 eV registrated in the XAS spectrum is higher than that obtained in the CIS experiment and by theoretical calculations.

Similar to U systems the matrix-element calculations were performed for another actinide metal - *fcc* Pu. As in the case of U, the obtained results reveal a series of the solid-state Cooper minima (Fig. 2) with the lowest-energy one located at 97 eV in a vicinity of the Pu $5d \rightarrow 5f$ excitation. The presented results have severe consequences for the interpretation of resonant PE data taken for solid systems with overlaping CM and Fano resonances in particular if details of the Fano profile are intended to be studied.

This work was supported by the Bundesministerium für Bildung und Forschung (BMBF), project no. 05 625 ODA; the Deutsche Forschungsgemeinschaft, Sonderforschungsbereich 463, TPB4 and TPB11, and Graduiertenkolleg "Struktur und Korrelationseffekte in Festkörpern".

---

* on leave from Institute of Physics, St. Petersburg State University, 198904 St. Petersburg, Russia

[1] U. Fano, Phys. Rev. **129**, 1866 (1961).
[2] A.Zangwill and P.Soven, Phys. Rev. Lett. **45**, 204 (1980).
[3] A.Zangwill and D.A.Liberman, Phys. Rev. B **36**, 6705 (1987); D.D.Sarma *et al.*,*ibitem* **36**, 2916 (1987).
[4] S. L. Molodtsov *et al.*, Phys. Rev. Lett. **78**, 142 (1997).
[5] C. Laubschat *et al.*, Phys. Rev. Lett. **65**, 1639 (1990).
[6] J. W. Allen, O. Gunnarsson, and K. Schönhammer, Advances in Physics **35**, 275 (1986).
[7] B. Reihl *et al.*, Phys. Rev. B **32**, 3530 (1985).
[8] J. W. Allen *et al.*, Phys. Rev. Lett. **54**, 2635 (1985).
[9] A. J. Arko, D. D. Koelling, and B. Reihl, Phys. Rev. B **27**, 3955 (1983).
[10] G. R. Stewart, Rev. Mod. Phys. **56**, 755 (1984).
[11] W.D. Schneider *et al.*, Phys. Rev. B **28**, 2017 (1983); C. Laubschat *et al.*, Physica Scripta **41**, 124 (1990); E. Weschke *et al.*, Phys. Rev. B **44**, 8304 (1991); O. Gunnarsson and T.C. Li, Phys. Rev. B **36**, 9488 (1987); S.L. Molodtsov *et al.*, Phys. Rev. B **60**, 16435 (1999).
[12] For a review, see, e.g., *The Actinide: Electronic Structure and Related Properties*, edited by A. Freeman and J.B. Darby, Jr. (Academic, NY, 1974), Vol. 1; A.J. Arko *et al.*, Physica B **163**, 167 (1990); A.J. Arko *et al.*, Philos. Mag. B **75**, 603 (1997).
[13] S. L. Molodtsov *et al.*, Phys. Rev. B **57**, 13241 (1998); J. Boysen *et al.*, J. of Alloys and Comp. **275-277**, 493 (1998).
[14] J.W.Cooper, Phys. Rev. **128**, 681 (1962).
[15] J.J.Yeh and I.Lindau, *Atomic data and nuclear data tables*, **32**, Academic Press (1985).
[16] S.L. Molodtsov *et al.*, Phys. Rev. Lett. **85**, 4184 (2000).
[17] B. Reihl *et al.*, Phys. Rev. B **26**, 1842 (1982).
[18] M. Iwan, E. E. Koch, and F. J. Himpsel, Phays. Rev. B **24**, 613 (1981).
[19] L. E. Cox *et al.*, Phys. Rev. B **35**, 5761 (1987).
[20] G. Landgren *et al.*, Phys. Rev. B **29**, 493 (1984).
[21] S. V. Halilov *et al.*, J. Phys.: Condens. Matter **5**, 3859 (1993).
[22] I. Abbati *et al.*, Phys. Rev. B **32**, 5459 (1985); G. Rossi *et al.*, Phys. Rev. B **28**, 3031 (1983); R.J. Cole *et al.*, Phys. Rev. B **46**, 3747 (1992).

FIG. 1. Experimental valence-band PE spectra (solid lines through data points) and calculated EDC's (solid subspectra) of *hcp* U metal taken at different photon energies and normal-emission geometry. Inset represents calculated bands along the Γ-A direction compared with experimentally derived dispersions (solid circles).

FIG. 2. $\mid M^{r}_{5f \rightarrow \varepsilon g} \mid^2$ calculated for *hcp* U metal and UPd_3 as well as for *fcc* Pu metal at different $h\nu$. Inset shows the radial parts of wave functions of *hcp* U for initial ($5f$ at E_F) and final (εg at 55 eV and 94 eV above E_F) states.

FIG. 3. Experimental (open circles) and calculated (solid circles) intensity variations of the Fermi-level peak for *hcp* U (present study) and UPd_3 (experimental data from Ref. [17]) as a function of photon energy. Inset: XAS spectrum taken in partial electron yield mode with 1-eV electrons for *hcp* U.

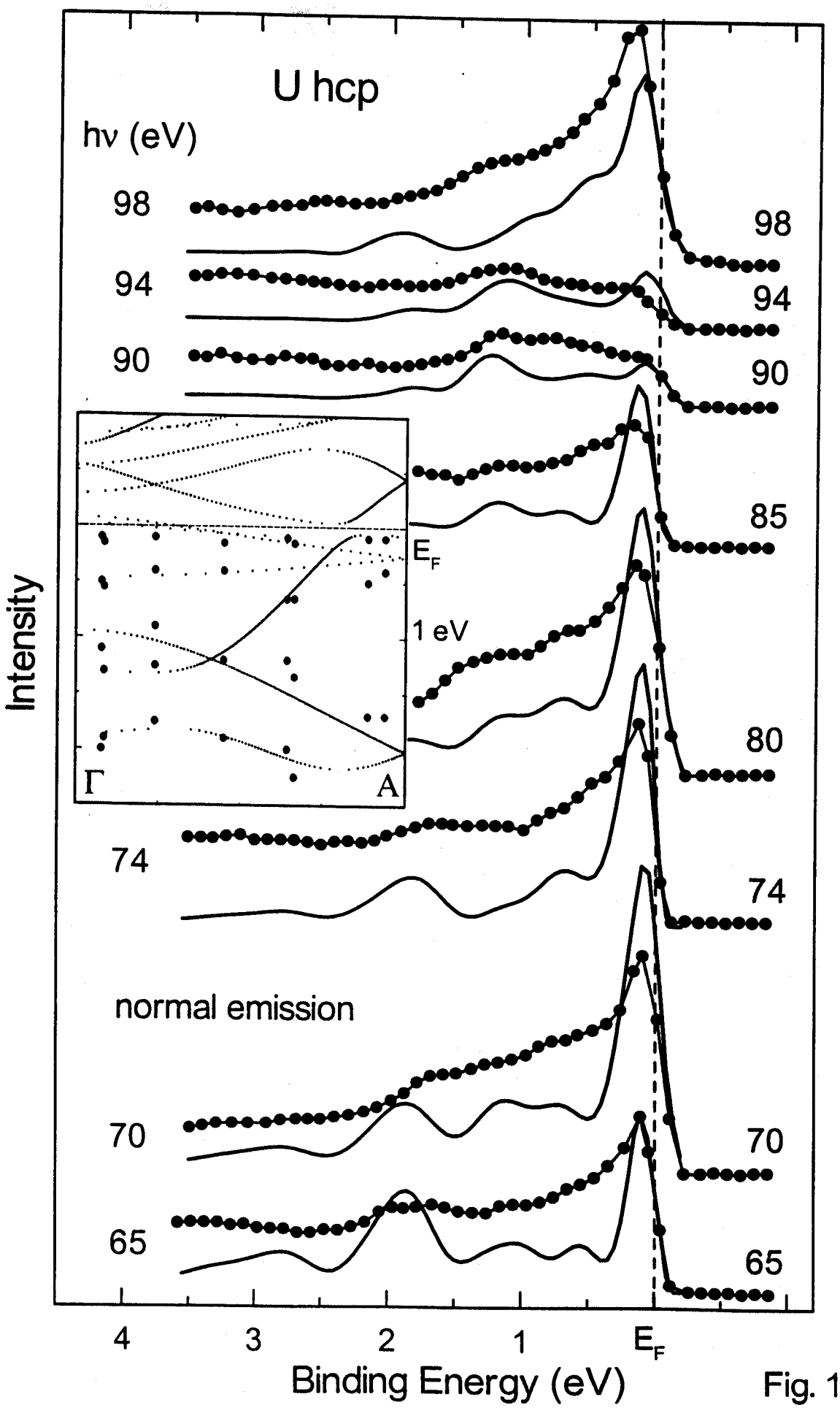
U hcp
hν (eV)
98
94
90
85
80
74
70
65
normal emission
E_F
1 eV
Γ
A
Intensity
4
3
2
1
E_F
Binding Energy (eV)

Fig. 1

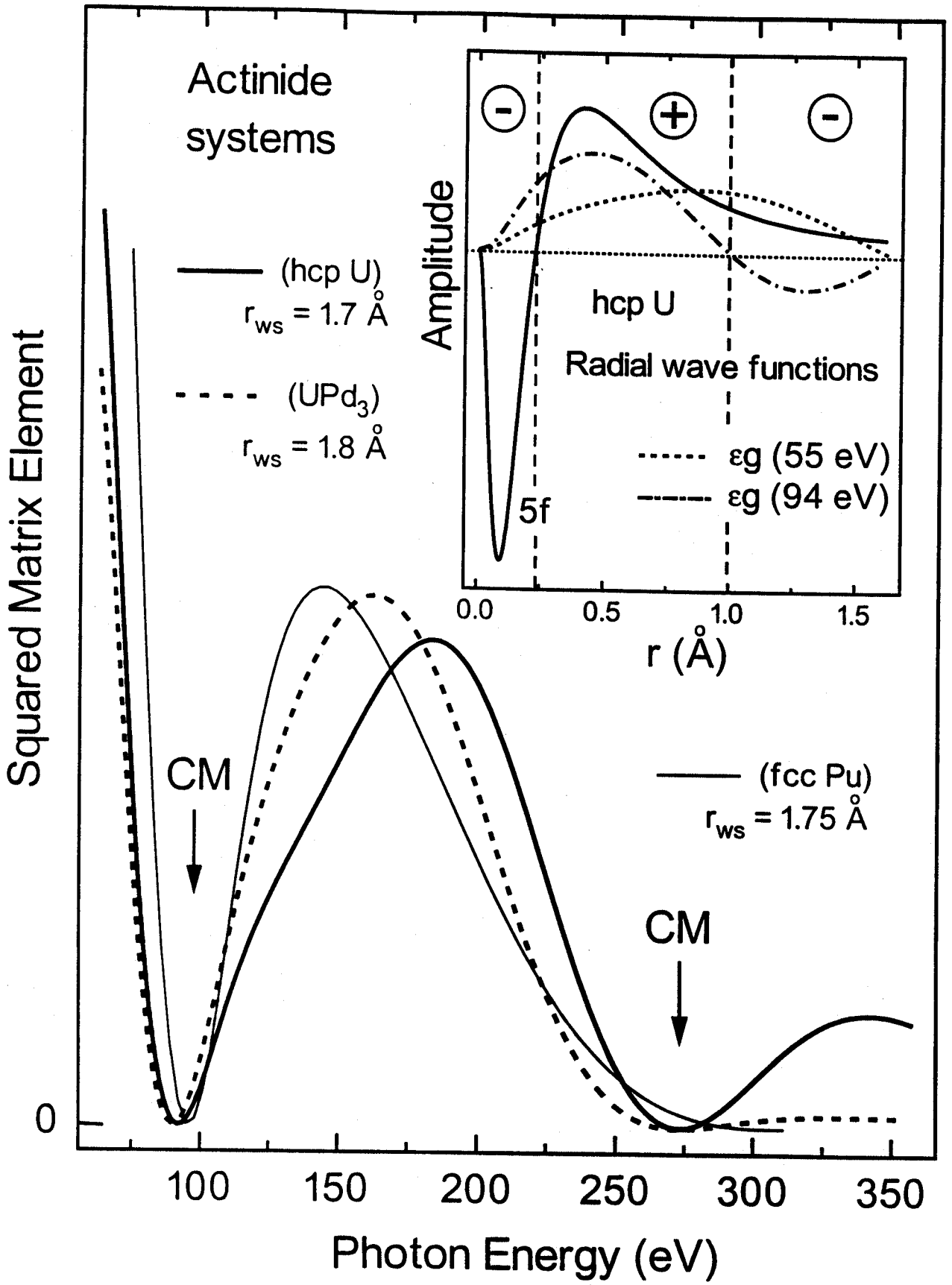
Actinide systems
(hcp U)
r_{ws} = 1.7 Å
(UPd$_3$)
r_{ws} = 1.8 Å
Amplitude
hcp U
Radial wave functions
εg (55 eV)
εg (94 eV)
5f
0.0
0.5
1.0
1.5
r (Å)
Squared Matrix Element
CM
CM
(fcc Pu)
r_{ws} = 1.75 Å
0
100
150
200
250
300
350
Photon Energy (eV)

Fig. 2

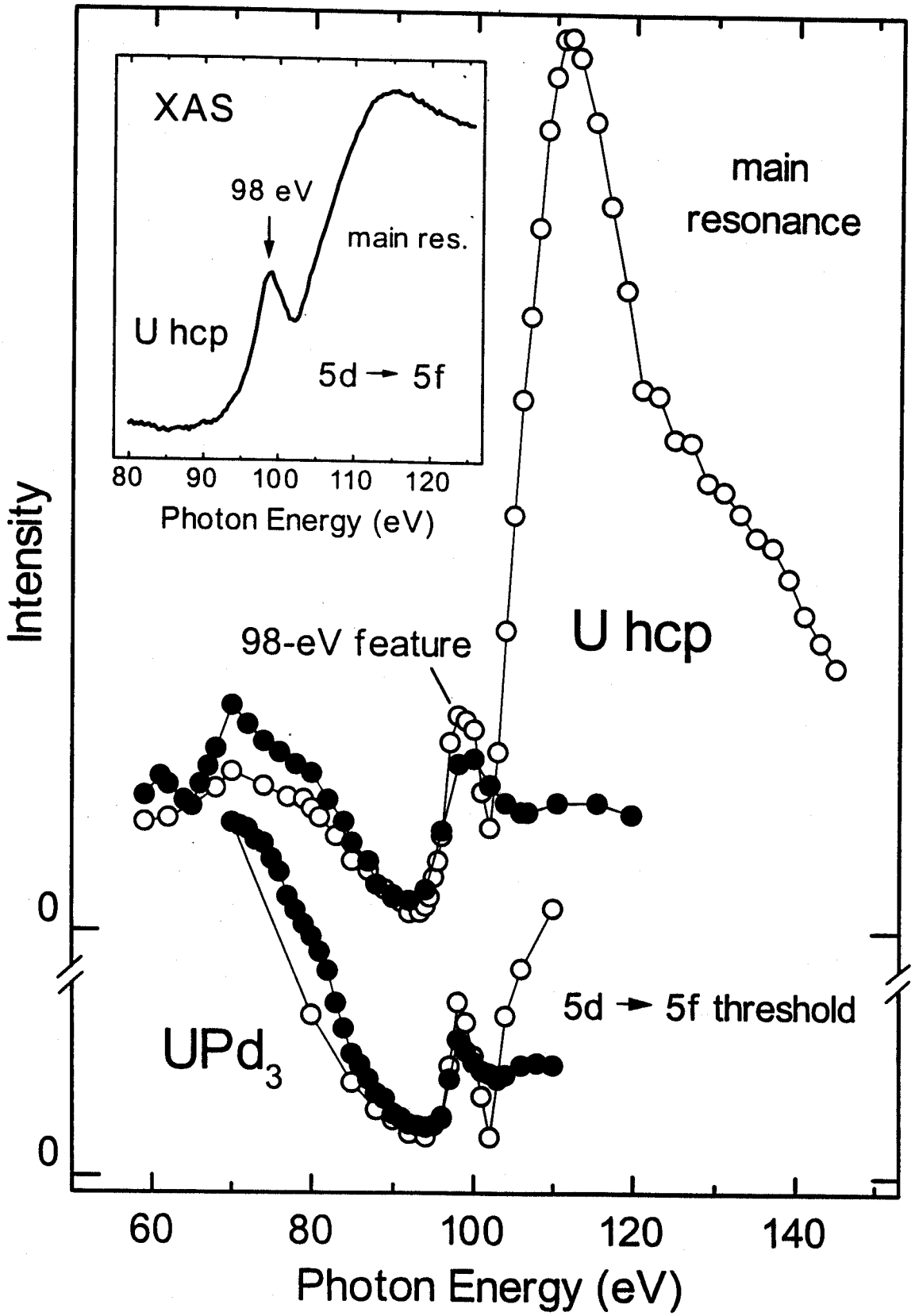
XAS
98 eV
main res.
U hcp
5d → 5f
80 90 100 110 120
Photon Energy (eV)
main
resonance
Intensity
98-eV feature
U hcp
0
5d → 5f threshold
UPd3
0
60 80 100 120 140
Photon Energy (eV)

Fig. 3